Colloids and Surfaces A 555 (2018) 473–481

Contents lists available at ScienceDirect

Colloids and Surfaces A

journal homepage: www.elsevier.com/locate/colsurfa

Environmentally friendly platforms for encapsulation of an essential oil: Fabrication, characterization and application in pests control

Natalia Sánchez-Arribas[a], Eduardo Guzmán[a,b,*], Alejandro Lucia[c,d], Ariel C. Toloza[c], Manuel G. Velarde[b], Francisco Ortega[a,b], Ramón G. Rubio[a,b,*]

[a] Departamento de Química Física, Facultad de Ciencias Químicas, Universidad Complutense de Madrid, Ciudad Universitaria s/n, 28040, Madrid, Spain
[b] Instituto Pluridisciplinar, Universidad Complutense de Madrid, Paseo Juan XXIII, 1, 28040, Madrid, Spain
[c] Centro de Investigaciones de Plagas e Insecticidas (UNIDEF-CONICET), Villa Martelli, Buenos Aires, Argentina
[d] Centro de Investigación en Sanidad Vegetal (CISaV), Facultad de Ciencias Agrarias y Forestales, UNLP, Calles 60 y 119, 1900, La Plata, Argentina

GRAPHICAL ABSTRACT

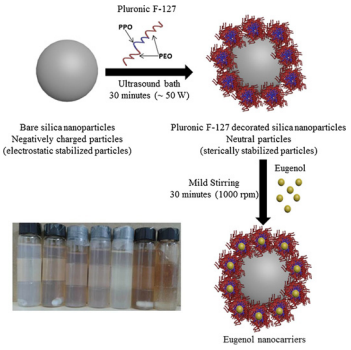

ARTICLE INFO

Keywords:
Essential oils
Nanoparticles
Colloidal dispersion
Biopesticides

ABSTRACT

Essential oils are highly volatile and non-water soluble natural products which have shown high efficiency against several insect pests. However, their low solubility in water is an important drawback for their practical applications. This work explores the design of new nanocarriers of eugenol based on silica nanoparticles capped with Pluronic F-127, a triblock copolymer of poly(ethylene oxide) and poly(propylene oxide). Dynamic Light Scattering (DLS) and ζ-potential measurements have shown that particles capped with Pluronic F-127 are able to disperse eugenol between the polymer chains, probably due to the presence of poly(propylene oxide) blocks. Thus, nanocarriers with a structure similar to Pluronic F-127 emulsions supported on silica nanoparticles are formed. These nanocarriers are only stabilized in aqueous medium under conditions in which the ratio between the weight fractions of Pluronic F-127 and eugenol is above 1.5, otherwise phase separation appears within the first 48 h after their preparation. Furthermore, the weight fraction of silica nanoparticles is limited to low values. This work offers new possibilities for designing new aqueous based formulations with application in pests control. The use of aqueous formulations for this purpose is interesting because it makes easy the application process, handling and storage, reducing the hazards for environmental and human health associated with the use of toxic and volatile solvent.

* Corresponding authors at: Departamento de Química Física, Facultad de Ciencias Químicas, Universidad Complutense de Madrid, Ciudad Universitaria s/n, 28040, Madrid, Spain.
E-mail addresses: eduardogs@quim.ucm.es (E. Guzmán), rgrubio@quim.ucm.es (R.G. Rubio).

https://doi.org/10.1016/j.colsurfa.2018.07.028
Received 17 April 2018; Received in revised form 17 July 2018; Accepted 17 July 2018
Available online 18 July 2018
0927-7757/

1. Introduction

Encapsulation of poorly water soluble substances is a promising tool for enhancing the availability of bioactive compounds with technological interest. Several storing and delivering systems formed by a core in which the drug is dissolved, a continuous aqueous phase and a shell protecting the drug has been described in the literature (particles, liposomes, emulsions) [1–4].

Essential oils can be considered among the molecules whose encapsulation and dispersion in aqueous medium presents an increasing interest [5]. This is due to their effectiveness against different insect pests because they are able to modify different aspects of their physiological function, including growth, reproduction or feeding. Moreover, essential oils may also act on the olfactory receptor, inducing attraction or repellency [6]. Furthermore, essential oils are highly volatile natural products, being their degradation in the environment faster than that of synthetic pesticides, which allows considering them a promising alternative for the preparation of more environmentally friendly formulations for pests control [7]. Therefore, the bioactivity of essential oils together with their negligible toxicity for mammals and environment have fostered the research on their potential applications on insect pests control [8–10]. Among essential oils, eugenol can be accounted among the most important. Eugenol is a phenylpropene, which is the major constituent of clove essential oil, also known as Turkish clove (*Syzygium aromaticum*) and shows interesting biological effects on several organisms [11]. The eugenol was reported to be effective as acaricide [12], insecticide [13], bacteriostatic or bactericide [14], fungicide [15], insect repellent [16], termiticide [17] and herbicide [18]. Furthermore, the eugenol is well known for its medicinal properties such as antiseptic, anti-inflammatory, antioxidant and anticonceptive [19,20].

Despite the numerous studies focused on the physico-chemical characterization of essential oils, their practical applications remains rather limited especially due to their poor solubility in water [21].This drawback has been partially solved by Lucia et al. [22] who prepared oil in water emulsions (O/W) to encapsulate several essential oils inside a shell of Pluronic F127, a triblock copolymer containing two lateral blocks of poly(ethylene oxide) and a central one poly(propylene oxide). Such formulations present a high water content (above 90 wt%) which limits significantly the dermal irritation associated with the contact between essential oils and the skin [23]. Furthermore, *in vitro* tests have shown the high effectiveness of such formulations against head lice (*Pediculus humanus capitis*). Another alternative to disperse essential oils in water is to take advantage of the so-called “ouzo effect” [24–28]. Other types of emulsions have been recently reported in order to increase the dispersion of essential oils in water for different applications, including agriculture, cosmetic and food science [29,30]. Another promising alternative prompt to explore for the encapsulation of essentials oils could be Pickering emulsions, in which the essential oil droplets will be protected by colloidal particles such as silica nanoparticles [31,32]. In most of the cases the stabilization of Pickering emulsion using silica nanoparticles requires the modification of the surface nature of the particles through physical [29,33,34] or chemical [35,36] methods due to the high hydrophilicity of silica. Pickering emulsions has been tested on the encapsulation and topical release of bioactive substance (trans-retinol and caffeine), and the results pointed out the important role on their activity of several physico-chemical parameter, e.g. physical nature of the stabilizing agent; pH, ionic strength and viscosity of the continuous phase; droplet size distribution; oil/water ratio and temperature [37,38]. However, there are no studies related to the application of Pickering emulsions in pests control.

This work studies a new alternative for the dispersion of eugenol in water by the use of polymer-decorated particles obtained by the non-covalent capping of silica nanoparticles with Pluronic F-127 chains. Thus, eugenol nanocarriers are obtained in which the Pluronic F-127 chains attached to the surface of silica nanoparticles form a shell around eugenol drops, favoring its dispersion in water. Silica nanoparticles may increase the effectivity of the formulation by clotting the pores of the exoskeleton through which insect take oxygen from air. Nanosilica systems have a wide range of applications, including microelectronics, disease diagnostics, optical communications, thin-film technology, and environmental and agricultural applications [39]. In the last years, several studies has reported the use of diatomaceous earth and silica nanoparticles as an alternative to chemical insecticides for pest control [40,41].

It is expected that the combination of essential oils with adjuvants (Pluronic F-127 and silica nanoparticles) may open new perspectives for the fabrication of aqueous-based formulations with enhanced efficiency in pests control, which present an environmentally friendly character. These new formulations are advantageous in relation to conventional insecticides in which one or several toxic compounds are included, because they provides the bases for reducing the potential hazards for human and environmental health associated with the use of solvents with high toxicity and volatility in commercial formulations. Thus, rendering to traditional systems for pests control toxic, difficult to store and handle, and unstable. It is expected that systems studied here can provide the bases for the fabrication of new formulations for pests control.

2. Materials and methods

2.1. Materials

Pluronic F-127 (Sigma-Aldrich, Germany) is a triblock copolymer, containing two lateral blocks of poly(ethylene oxide) with molecular weight 4.4 kDa and a central one of poly(propylene oxide) with a molecular weight around 3.8 kDa. Silica nanoparticles were purchased from Sigma-Aldrich (Germany) as a dispersion of Ludox® TMA colloidal silica with a solid content of 34 wt%. Eugenol (purity 99%) was purchased from Sigma-Aldrich (Germany). All the chemicals were used as received.

The cleaning of the glassware was carried out with a saturated solution of KOH in ethanol, followed by an abundantly rinsing with water of Milli-Q quality obtained using a multicartridge purification system (Younglin 370 Series, South Korea). The water obtained had a resistivity close to 18 MΩ·cm^{-1} and a total organic content lower than 6 ppb. The same water was used for the preparation of the solutions.

2.2. Eugenol nanocarriers preparation

Dispersions were prepared in tubular glass vials (10 mL) by weight using an analytical balance with precision of ± 0.1 mg. For this purpose, the method described by Lucia et al. [20] was slightly modified for introducing an additional component on the formulation: silica nanoparticles. The preparation of dispersions of Pluronic F-127-decorated silica nanoparticles was carry out directly in the vial by mixing the required amounts of an initial silica nanoparticles dispersion and the Pluronic F-127 solution. These mixtures were homogenized by sonication during 30 min (power ~ 50 W) prior adding the neccesary amount of eugenol to reach the desired weight ratio between the components. Afterwards, the mixtures were homogenized by stirring using a magnetic bar at 1000 rpm during 30 min. Sheme 1 represents a sketch describing the different steps of the fabrication process of eugenol nanocarriers.

2.3. Methods

A Zetasizer Nano ZS instrument (Malvern Instruments Ltd., Worcestshire, UK) was used for Dynamic Light Scattering (DLS) experiments using radiation corresponding to the red line of a He-Ne laser (wavelength, $\lambda = 633$ nm) in quasi-backscattering configuration (scattering angle, $\theta = 173°$). All the samples were filtered before the

Fig. 1. a) Pluronic F-127 aqueous solutions with weight fractions in the 2–20 wt% range. Notice that the viscosity of the solutions increases with the weight fraction of Pluronic F-127. b) Detail of the solution with Pluronic F-127 weight fraction ~ 20 wt%. c) Mixed dispersions containing fix silica nanoparticles concentration (~ 1 wt%) and increasingly amounts of Pluronic F-127 (2–20 wt% range). Notice that the increase of Pluronic F-127 weight fraction leads to an increase on the viscosity of the dispersions. d) Detail of the mixed silica nanoparticles - Pluronic F-127 dispersion containing a weight fraction of copolymer ~ 20 wt%.

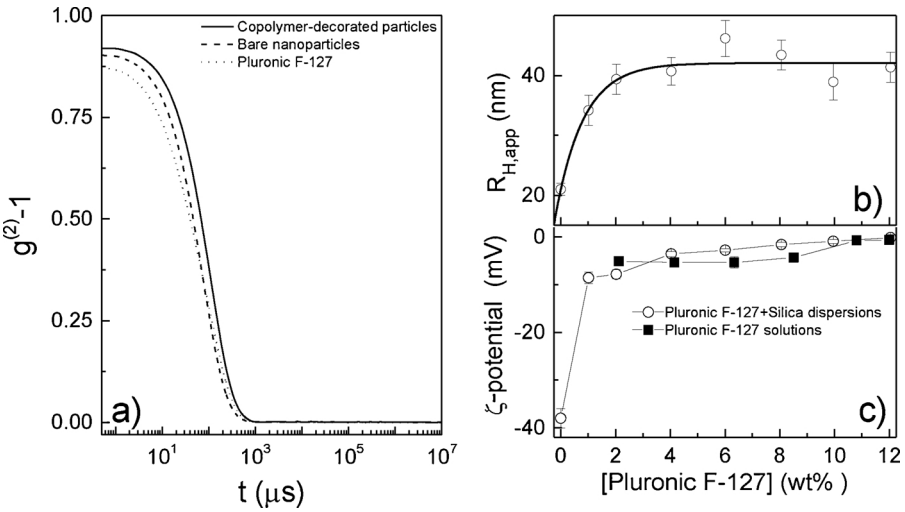

Fig. 2. (a) Normalized intensity autocorrelation function obtained by DLS for a Pluronic F-127 solution and bare and copolymer-decorated nanoparticles dispersions. Notice that Pluronic F-127 in the solution and in the copolymer-decorated nanoparticles dispersion is 6 wt%, i.e. in the sol region. (b) Dependence of the hydrodynamic radius ($R_{H,\ app}$) of copolymer decorated on the weight fraction of Pluronic F-127. The lines are guides for the eyes. (c) ζ-potential dependence on the weight fraction of Pluronic F-127. For sake of comparison the results corresponding to the ζ-potential of Pluronic F-127 solutions are also shown. The lines are guides for the eyes.

measurements, in a clean-room, using a Nylon membrane with a pore diameter of 0.45 μm (Millex; Millipore, Billerica, MA, USA). This allows removing possible dust particles in the samples. The measurement were carried out using optical glass cell (Hellma®6030-OG Model; Hellma, Jena, Germany). In DLS experiments, the normalized intensity autocorrelation function, $g^{(2)}(q, t)$, follows an exponential decay with time. In the simplest case to the Brownian motion of monodisperse objects

$$g^{(2)}(q, t)-1 = \beta e^{-2t/\tau} = \beta e^{-2Dq^2t} \quad (1)$$

with t is the time, τ the characteristic relaxation time which is directly related to the diffusion coefficient (D), $q = \frac{4\pi n}{\lambda} sin\left(\frac{\theta}{2}\right)$ the wavevector, and n the solution refractive index which was assumed to be close to that of the continuous phase ($n = 1.33$) and β, which is close to 1, is the coherence factor. For spherical particles diffusing in a continuous Newtonian medium, D can be assumed to follow the Stoke-Einstein relationship

$$D = \frac{k_B T}{6\pi\eta R_{H,app}} \quad (2)$$

where k_B and T are the Boltzmann constant and the absolute temperature, η is the viscosity of the continuous phase, and $R_{H,app}$ is the apparent hydrodynamic radius of the particles in suspension. Three replicas of each measurement were carried out, being the deviation between the different replicas less than 1%.

Electrophoretic mobility, μ_e, measurements were carried out for obtaining the zeta potential, ζ-potential, using also the Zetasizer Nano ZS instrument (Malvern Instruments Ltd., Worcestshire, UK) The measured μ_e values were transformed into ζ-potential by the Smoluchowski's relation. The accuracy in the determination of the ζ-potential was better than ± 5 mV.

The turbidity of the samples was determined measuring the transmittance of the mixtures at 400 nm using a UV/visible spectrophotometer (HPUV 8452) [42]. The turbidity was obtained as

$$Turbidity = 1-\frac{T(\%)}{100} \quad (3)$$

3. Results and discussion

3.1. Characterization of the silica dispersions and Pluronic F-127 solutions

The first step of the study is to understand the behavior of bare silica nanoparticles and Pluronic F-127 in aqueous medium. Silica nanoparticles present an average apparent hydrodynamic radius ($R_{H,\ app}$) about 21.0 ± 0.2 nm as was determined by DLS, and are negatively charge (ζ-potential ~ -38 ± 2 mV) due to the dissociated silanol groups on their surface which prevents their aggregation in water.

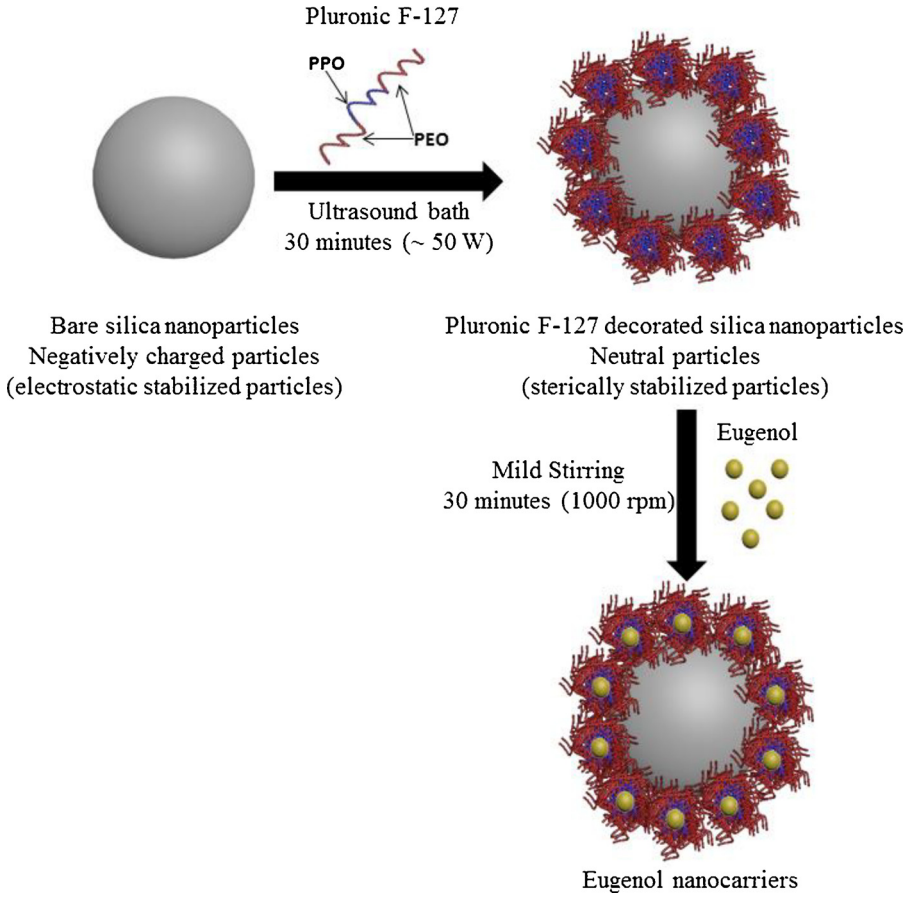

Scheme 1. Sketch describing the different steps of the fabrication process of eugenol nanocarriers.

Fig. 3. Dispersions of eugenol in aqueous Pluronic F-127-decorated nanoparticles (Pluronic F-127 2 wt% and silica nanoparticles 1 wt%) with increasingly eugenol concentrations (from left to right: 1–10 wt%): as prepared (a) and after 48 h (b). The values of $R_{plu/eug}$ represented (from left to right) are: 1.56, 0.86, 0.65, 0.46, 0.37, 0.31, 0.26, 0.22, 0.20 and 0.18.

However, the negative charge cannot rule out the existence of non-dissociated silanol groups, which can interact through hydrogen bond with the ethoxy groups existing in Pluronic F-127 chains.

In order to follow with the characterization of the bare materials, Pluronic F-127 with increasing concentrations were studied. Fig. 1a shows a sequence of images of aqueous solutions of Pluronic F-127 with increasing weight fractions. Notice that in all the solutions, the copolymer content is above the critical micellar concentration (cmc ~ 0.5 wt%) [43].

Pluronic F-127 solutions show increasingly viscosity with the weight fraction of copolymer. This increase is especially evident from copolymer weight fraction values about 12 wt%, leading to a sol-gel transition when the weight fraction of copolymer in solution is about a 20 wt% (see Fig. 1b). This sol-gel is in agreement with previous studies in the literature for different polymer of the Pluronic family [44,45], and reduces the range of Pluronic F-127 concentrations with can be useful on the preparation of eugenol nanocarriers.

3.2. Capping silica nanoparticles with Pluronic F-127

The interaction of Pluronic F-127 and silica nanoparticles is expected to lead to the formation of copolymer-decorated silica nanoparticles through the formation of hydrogen bonds between the non-dissociated silanol groups at the nanoparticles surface and the ethoxy groups on the copolymer, in a similar way to that described for other polymers of the Pluronic family [46]. The formation of hydrogen bond between the copolymer and silica is supported on their strength, being these hydrogen bonds 25–30 % stronger than those formed by silanol groups and water [47]. Thus, the replacement of water molecules for the copolymer chains is expected once Pluronic F-127 is added to dispersion of silica nanoparticles. Fig. 2c shows a sequence of images of mixed dispersions containing a fix concentration of silica nanoparticles (~ 1 wt%) and increasing concentrations of Pluronic F-127.

The results evidence again the sol-gel transition as the Pluronic F-127 concentration increases. However, the addition of nanoparticles and the formation of copolymer-decorated nanoparticles leads to a prior increase of the system viscosity in relation to that occurring for Pluronic F-127 solutions (around 10 wt% against the 12 wt% found in

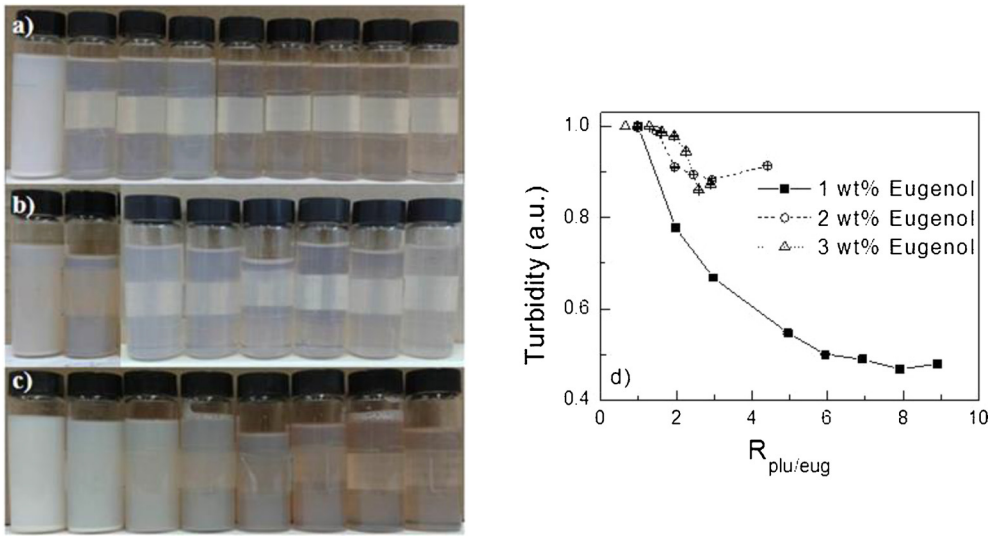

Fig. 4. (a), (b) and (c) Aqueous dispersions of eugenol nanocarriers prepared using a fixed silica nanoparticles concentration (1 wt%) and different Pluronic F-127 concentrations (varying in the three panels from left to right from 1 wt% to 9 wt%). Each panel shows nanocarriers dispersions containing different different eugenol content: 1 wt% (a), 2 wt% (b) and 3 wt% (c). (d) Turbidity dependences on $R_{plu/eug}$ for dispersions shown in panel (a), (b) and (c). Note that samples with turbidity close to 1 appear as phase separated mixtures.

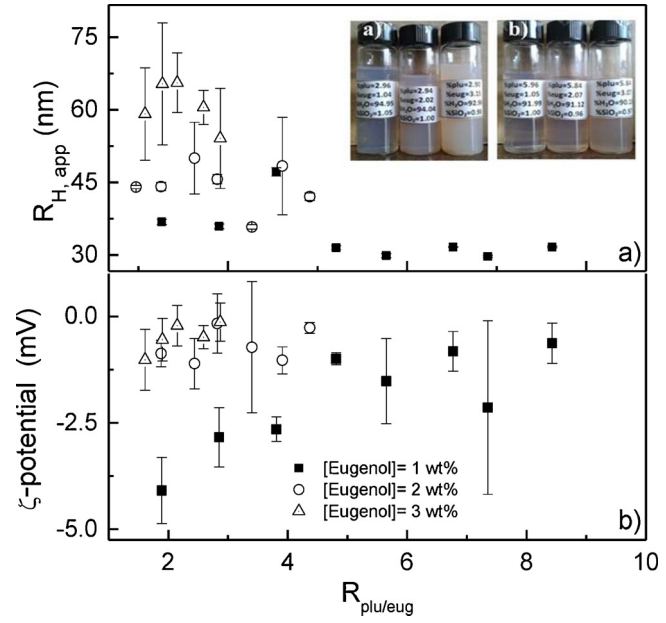

Fig. 5. $R_{H,\ app}$ (a) and ζ-potential (b) dependences on $R_{plu/eug}$ for dispersions containing fixed concentrations of silica nanoparticles (~ 1 wt%) and increasingly concentrations Pluronic F-127. The results show three different eugenol concentrations (from 1 wt%, 2 wt% and 3 wt%). The inserted images in panel (a) show dispersions containing fixed concentrations of silica nanoparticles (~ 1 wt%) and of Pluronic F-127 (3 wt%, panel (a) and 6 wt% panel (b)) and increasingly concentrations of eugenol (from 1 wt% to 3 wt%, from left to right).

Pluronic F-127 solutions). This is explained considering that the nanoparticles take out part of the free volume accessible in the liquid [48], such excluded volume leads to the formation of cross-linked networks of Pluronic F-127 chains for copolymer weight fractions lower than that found in pure Pluronic F-127 solutions. This behavior further reduces the Pluronic F-127 weight fraction region interesting on the fabrication of nanocarriers.

DLS provides confirmation of the formation of copolymer-decorated nanoparticles. Fig. 2a shows for the sake of example the normalized intensity autocorrelation functions obtained by DLS for Pluronic F-127 solutions, bare nanoparticles and copolymer-decorated particles dispersions.

The results show that the characteristic relaxation times for nanoparticles and Pluronic F-127 are in the same time scale. Thus, according to Eqs. (1) and (2) it is possible to assume that polymer micelles and nanoparticles present similar hydrodynamic radius. It is worth mentioning that the autocorrelation function for Pluronic F-127 seems to be more complex than that corresponding to nanoparticles dispersion. This could be explained considering that copolymer solutions contain more than one component: free polymer chains and polymer micelles. When the dispersions of copolymer decorated particles are considered, the autocorrelation function is shifted to higher times, which means that the scatterers have bigger size, due to the adsorption of polymer chains onto the nanoparticles surface. For a deeper understanding of the adsorption of polymer onto silica nanoparticles DLS and ζ-potential measurements were carried out for dispersions with fixed nanoparticle concentration and increasingly Pluronic F-127 weight amount. Fig. 2b and c shows the Pluronic F-127 weight fraction dependence of the apparent hydrodynamic radius and ζ-potential of the mixed dispersions.

The addition of Pluronic F-127 to silica nanoparticles dispersions leads to a sharp increase on the hydrodynamic radius of the nanoparticles from values around 21 nm for the bare particles up to values of about 40 nm. This increase of the $R_{H,app}$ could be considered a signature of the adsorption of Pluronic F-127 micelles onto the nanoparticles surfaces (Note that the size of the copolymer micelles is around 20 nm). The adsorption of Pluronic F-127 micelles onto hydrophilic surfaces has been reported to be favored in relation to the micellation process occurring in the bulk [49,50]. For the case of ζ-potential values, it is found a shift from values around −40 mV to values close to the electroneutrality. This means that the adsorption of a thick layer of Pluronic F-127 leads to the shielding of the negative charge present on the particle surface. Thus, particles go from electrostatic stabilization to a steric one (see Scheme 1).

3.3. Fabrication of nanocarriers of eugenol

We have described in a previous publication the preparation of essential oils in water emulsions only stabilized by Pluronic F-127 [20]. These emulsions present mortality in the range 40–60 % when they were tested against head lice. This effectiveness was strongly depending on the nature of the essential oil used. However, it is known that conventional emulsions have no long-term stability since they are metastable systems. It is expected that the use of nanoparticles can help to enhance the stability of the formulations. It has been discussed above that Pluronic F-127 can adsorb onto particles surfaces thus modifying their hydrophobicity of the particles. In this work, we have worked under conditions in which the eugenol content of the formulations is

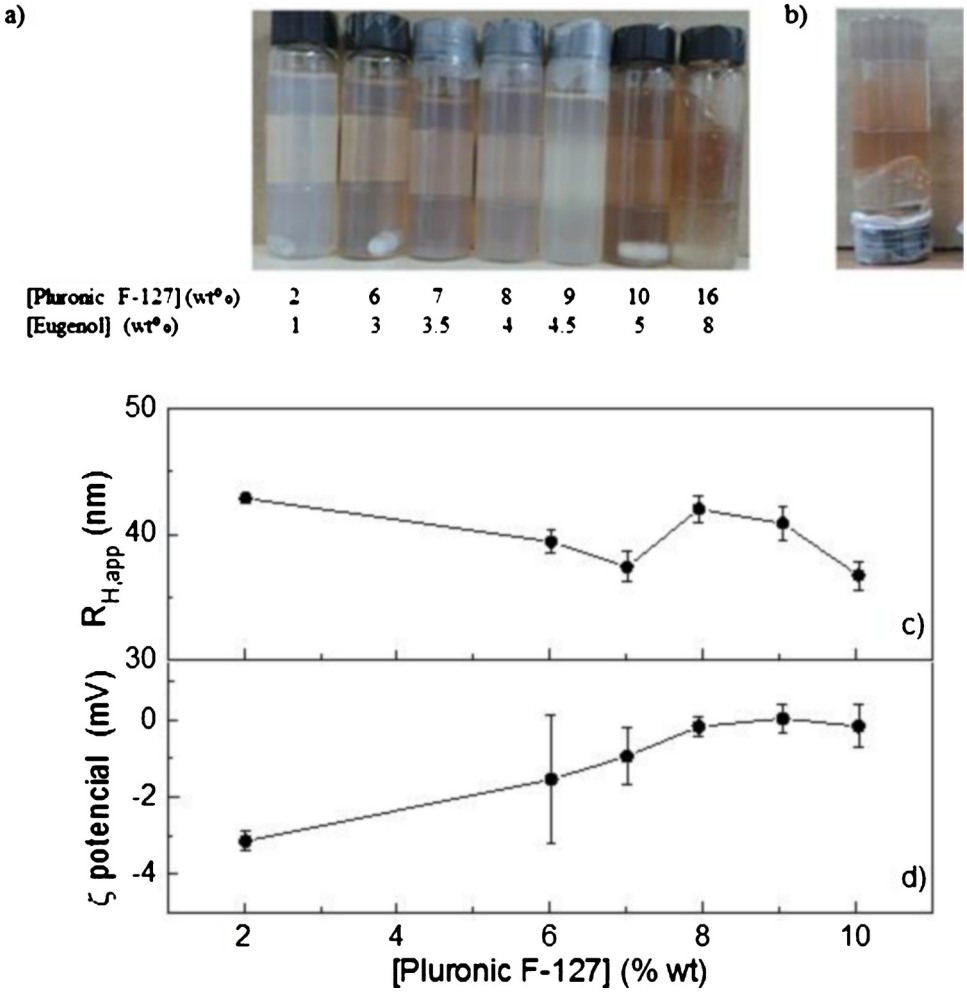

Fig. 6. (a) Dispersions containing a fixed value of $R_{plu/eug}$ ~ 2, obtained with increasing concentrations of Pluronic F-127 and eugenol. (b) Detail of the mixtures containing $R_{plu/eug}$ ~ 2, obtained with concentrations of Pluronic F-127 and eugenol, around 12 wt% and 6 wt% (right), and 16 wt% and 8 wt% (left), respectively. Note the gel-like character of such samples. (c) $R_{H,app}$ dependence on Pluronic F-127 for samples with $R_{plu/eug}$ ~ 2 containing a constant amount of silica nanoparticles (~ 1 wt%). The line is a guide for the eyes. (d) ζ-potential dependences on Pluronic F-127 for samples with $R_{plu/eug}$ ~ 2 containing a constant amount of silica nanoparticles (~ 1 wt%). The line is a guide for the eyes.

relatively low, and. the results show that, under certain conditions, copolymer-decorated nanoparticles are able to disperse eugenol in water.

The first step in the fabrication of nanocarriers is to determine the optimal compositions to obtain stable dispersions of eugenol in water. For this purpose, the concentration of silica nanoparticles and copolymer were fixed in 1 wt% and 2 wt%, respectively, and the eugenol concentration was increased gradually from 1 to 10 wt%. This allows us to define as control parameter the ratio between the weight fractions of Pluronic F-127 and eugenol, $R_{plu/eug}$. In our previous work, we showed that such ratio allows stabilizing emulsions for values above a threshold value about 1.56. Therefore, this value could be considered optimal for the dispersion of eugenol in Pluronic F-127 shells. Fig. 3 shows a series of images of dispersions, with different values of $R_{plu/eug}$.

Fresh prepared dispersions (Fig. 3a) show a more milky aspect as the value of $R_{plu/eug}$ decrease, i.e. as the amount of eugenol is increased. This is associated with a less effective dispersion of eugenol between the Pluronic F-127 chains, leading to the coalescence of the drops and the subsequent phase separation as it is observed from the images of the dispersions after 48 h (Fig. 3b) where in most cases the formation of a solid precipitate is observed on the bottom of the vial. Only, the sample with a value of $R_{plu/eug}$ close to 1.56 (first suspension from the left in both panels of Fig. 3) remains as one phase dispersion, providing the bases for the development of eugenol nanocarriers.

Once the existence of a threshold value for $R_{plu/eug}$ is known, the analysis of the eugenol dispersion in the copolymer-decorated particles dispersion was analyzed for three different weight fraction of eugenol (1, 2 and 3 wt%). The choice of such small contents allows avoiding potential dermal irritation effects associated with the use of essential oils in real formulations. Fig. 4 shows the images for suspensions prepared with the three eugenol concentrations and different Pluronic F-127 concentrations in the range 1–9 wt%. Thus, it is possible to modify the value of $R_{plu/eug}$.

The results show that, for the lowest Pluronic F-127 dispersions, phase separated milky dispersions with the appearance of a precipitate in the bottom of the vials are obtained. This is especially true for those mixtures containing lower amounts of copolymer, i.e. lower values of $R_{plu/eug}$. The appearance of phase separation is particularly evident as the concentration of eugenol is increased, being the phase separation region extended up to higher values of the Pluronic F-127. In order to quantify the degree of phase separation, turbidity measurements were carried out. Fig. 4d shows the turbidity measurements carried out for samples shown in Fig. 4a–c. The results show that samples with values of $R_{plu/eug}$ below 1.5–2 present high values of turbidity in agreement with the presence of phase separation. The turbidity shows that the increase of $R_{plu/eug}$ enhances the dispersion of eugenol within the aqueous phase. This could be explained considering that a higher amount of Pluronic F-127 in relation to the amount of eugenol leads to the formation of more rigid Pluronic F-127 shell coating the eugenol drops. It is worth mentioning that for the highest eugenol concentrations, the dispersions present higher turbidity, this can be explained as a consequence of change in the optical density of the dispersions associated with the increase of the number or the size of eugenol drops. The increase of the turbidity with the eugenol content is clearly evidenced from the inserted images in Fig. 5a.

The changes on the turbidity of the samples as the eugenol

concentration increases can be explained on the bases of the results obtained by DLS measurements. Fig. 5 shows the dependences of $R_{H,\ app}$ and ζ-potential on the value of $R_{plu/eug}$.

The results that for fixed eugenol concentrations, there are no dependences of the nanocarriers size ($R_{H,\ app}$) on the value of $R_{plu/eug}$ (Fig. 5a), i.e. on the Pluronic F-127 concentration, being the average values of $R_{H,\ app}$ about 60, 45 and 30 nm for 3, 2 and 1 wt% of eugenol, respectively. This points out a increase of the size of the nanocarriers with the eugenol concentration. This could be explained assuming that the increase of the eugenol for fixed values of $R_{plu/eug}$ requires the formation of more expanded copolymer structure in order to allow the accomodation of the higher oil amount. When the ζ potential of the nanocarriers is analyzed, values close to zero were found within the whole set of studied samples, which is again a result of the shielding of the surface charge of the silica nanoparticles due to the adsorption of the Pluronic F-127.

The above results concern so far to the optimization of the conditions for the fabrication of eugenol nanocarriers. From the results, we found that maintaining $R_{plu/eug}$ in values larger of 1.5 it is possible to prepare stable dispersions of nanocarrier. Focusing our attention on samples in which the value of $R_{plu/eug}$ is maintained constant by the simultaneous increasing of Pluronic F-127 and eugenol, it is possible to understand the limitation of the dispersion of eugenol using nanocarriers, i.e. the maximum amount of eugenol that can be dispersed using particles capped with copolymer without the appearance of phase separation or gellification. This presents interest because it might provide the bases for optimizing the dose of eugenol encapsulated. Fig. 6 shows dispersions with $R_{plu/eug} \sim 2$, presenting increasingly amounts of Pluronic F-127 and eugenol.

The images show that the increase of the Pluronic F-127 and eugenol concentration leads to the transition from a sol-like state to a gel-like state, in which the eugenol drops are dispersed into a viscous matrix. This sol-gel transition reduces the maximum amount of eugenol dispersed in aqueous solution. It is worth to mention that the gellification process is found for Pluronic F-127 concentrations lower than in water dispersions. This could be explained at least partially due to the contribution to the viscosity associated with the presence of eugenol, which presents a viscosity almost one order or magnitude larger than that corresponding to water. It is important to note that the gel-like mixtures present less interest for the fabrication of platform for encapsulation and controlled release of active ingredients in applications associated with pests control because gels limit the dispersion of the active ingredient to the environment. However, they can be useful for the fabrication of other technological materials, especially in those cases in which a sustained release of the active compound is required, e.g. systems for topical applications [51]. DLS experiments and ζ-potential measurements were carried out within the region corresponding to aqueous dispersions (see Fig. 6c and d). The results do not show any dependence neither of the $R_{H,app}$ nor of the ζ potential on the Pluronic F-127 concentration

3.4. Effect of the silica concentration on nanocarriers preparation

The above results concern so far to the stabilization of nanocarriers with a fixed amount of silica nanoparticles (~ 1 wt%), controlling the dispersion of eugenol through the value of $R_{plu/eug}$. This section describes briefly the effect of the concentration of silica nanoparticles on the preparation of the nanocarriers. Fig. 7 shows the effect of the increase of silica concentration, in the 0.1–20 wt% range, on the stabilization of nanocarriers with fixed $R_{plu/eug} \sim 2$.

The results show that the increase of the silica nanoparticles concentration drives the system into the two phase region, it can be concluded that only dispersions with a maximum content of silica about 1 wt% are stable, whereas solid precipitates are observed in those containing about 5 wt%. This is because of the increase of the silica nanoparticles increase the surface area in which Pluronic F-127 can

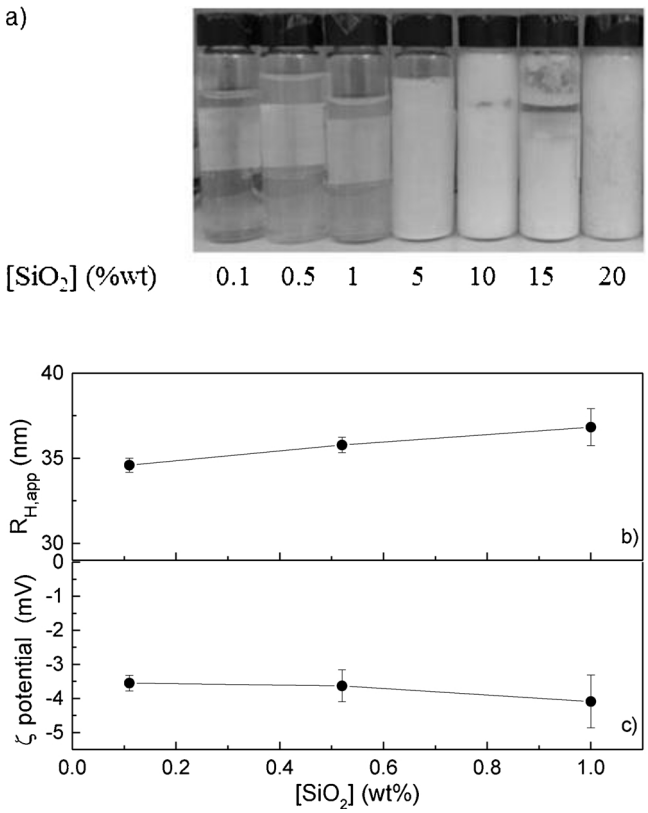

Fig. 7. a) Dispersions containing a fixed value of $R_{plu/eug} \sim 2$ and increasing amount of silica nanoparticles. $R_{H,app}$ (b) and ζ potential (c) dependences on silica nanoparticles concentration for samples with $R_{plu/eug} \sim 2$ within the liquid region. The lines are guides for the eyes.

adsorb, therefore, the surface concentration of copolymer is not be enough to lead to a steric stabilization of the particles, even if the neutralization of the surface charge is reached. However, the eugenol seems to be dispersed independently of the nanoparticle concentration. Therefore, it is possible to assume that the limiting factor for the eugenol dispersion is the $R_{plu/eug}$ value. Fig. 7b and c show that for stable dispersions the size and charge of the nanocarries is not modified by the increase of the nanoparticles concentration. These results allows confirming that the use of low particles concentrations is recommended for the fabrication of nanocarriers.

3.5. Conventional emulsions vs. eugenol nanocarriers

In our previous publication [20], we have discussed the possibility to stabilize emulsions of essential oils using only Pluronic F-127. Here, we discuss the results obtained for a set of concentional emulsions and nanocarriers with similar concentration of eugenol and copolymer. Fig. 8 shows the $R_{H,app}$ and ζ potential for both type of systems.

The results shows that in both cases the Pluronic F-127 shell guarantee a steric stabilization of the eugenol on the dispersion (ζ potential values close to 0). Furthermore, the DLS measurements shows the increase of the size of the dispersed objects when silica nanoparticles are included in the medium.

3.6. Nanocarriers as insecticides

In our previous publication [20], we analyze the effectivity of essential oil in water emulsions against head lice (*Pediculus humanus capitis*) following the procedure described in references [52,53]. The different emulsions obtained induce lice mortality in the 30–67 % range; in particular emulsions containing eugenol present mortality

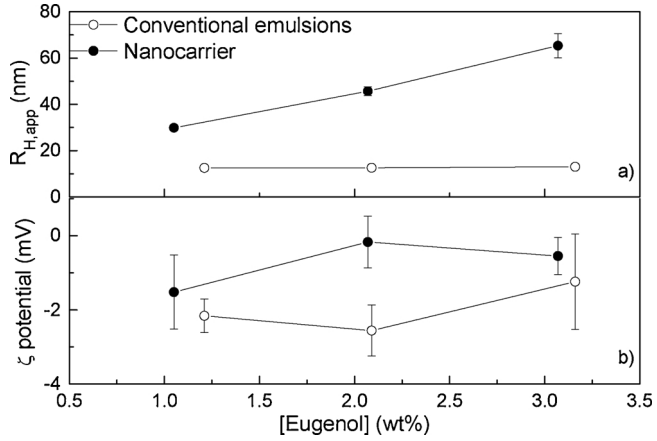

Fig. 8. $R_{H,app}$ (a) and ζ potential (b) dependences on eugenol concentration for dispersions containing ~6 wt% of Pluronic F-127, in absence (open circles) and presence (close circles) of ~ 1 wt% of silica nanoparticles. The lines are guides for the eyes.

around 52%. The inclusion of silica nanoparticles to fabricate nanocarriers allows us to enhance the effectivity of the formulations leading to values about 60% of mortality.

Furthermore, the eugenol is considered safe and not acutely toxic, with an oral LD_{50} of 2680 mg/kg bw in rat [54] and 3000 mg/kg bw in mouse [55]. However, it is slightly irritant for eyes and skin depending on the formulation. On the other side, eugenol is considered among the products that are exempt from the requirements of the Federal Insecticide, Fungicide, and Rodenticide Act (FIFRA-EPA) regulations. The Drug Authority of USA (FDA) categorized the eugenol as Generally Recognized As Safe (GRAS) for use in dental cement or as a food additive. Thus, it is possible to assume that the obtained nanocarriers present a potential application on the development of new formulations for pest control.

4. Conclusions

This work has been focused on the fabrication of new eugenol nanocarriers based on Pluronic F-127 capped silica nanoparticles. The results have pointed out that the preparation of new nanocarriers is mainly limited by two different factors, the first one the ratio between the amount of Pluronic F-127 and the eugenol one ($R_{plu/eug}$). This is because eugenol droplets need minimum polymer content for their dispersion in water. In the systems studied, this optimum $R_{plu/eug}$ value is above 1.5. The size of the nanocarriers do not depend neither of the Pluronic F-127 content nor of the silica nanoparticles concentration, but it can be tuned changing the eugenol concentration due to their effect on the spread of the copolymer chains. This type of nanocarriers was tested in bioassays against lice (*Pediculus humanus capitis*), presenting a high effectiveness, leading to death rates about 60%, gathering important possibilities on their application on pest control. All components used in this system are biocompatible. This can help to reduce the problems associated with the application process, handling and storage of commercially available formulations for pests control, limiting the hazards for environmental and human health related the use of toxic and volatile dispersing solvent. Furthermore, it would be possible to use the nanocarriers obtained for applications in other fields such as pharmacology or drug delivery. Moreover, gel formulations obtained could also useful in several technological fields.

Conflict of interest

The authors declare that they have no conflict of interest.

Acknowledgements

This work was funded by MINECO under grants CTQ2016-78895-R. AL and ACT received funding from Agencia Nacional de Promoción Científica y Técnica (ANPCyT)PICT 2016-1111, and Universidad CAECE. We are grateful to C.A.I. Espectroscopia from the UCM for the use of their facilities.

References

[1] D.R. Dias, D.A. Botrel, R.V.D.B. Fernandes, S.V. Borges, Encapsulation as a tool for bioprocessing of functional foods, Curr. Opin. Food Sci. 13 (2017) 31–37.
[2] G. Chen, Y. Xie, R. Peltier, H. Lei, P. Wang, J. Chen, Y. Hu, F. Wang, X. Yao, H. Sun, Peptide-decorated gold nanoparticles as functional nano-capping agent of mesoporous silica container for targeting drug delivery, ACS Appl. Mat. Interfaces 8 (2016) 11204–11209.
[3] E. Guzmán, A. Mateos-Maroto, M. Ruano, F. Ortega, R.G. Rubio, Layer-by-Layer polyelectrolyte assemblies for encapsulation and release of active compounds, Adv. Colloid Interface Sci. 249 (2017) 290–307.
[4] E. Guzmán, R. Chuliá-Jordán, F. Ortega, R.G. Rubio, Influence of the percentage of acetylation on the assembly of LbL multilayers of poly(acrylic acid) and chitosan, Phys. Chem. Chem. Phys. 13 (2011) 18200–18207.
[5] M.D.L. Moretti, G. Sanna-Passino, S. Demontis, E. Bazzoni, Essential oil formulations useful as a new tool for insect pest control, AAPS PharmSciTech 3 (2002) 64–74.
[6] A. González-Coloma, C. López-Balboa, O. Santana, M. Reina, B.M. Fraga, Triterpene-based plant defenses, Phytochem. Rev. 10 (2011) 245–260.
[7] J.B. Pillmoor, K. Wright, A.S. Terry, Natural products as a source of agrochemicals and leads for chemical synthesis, Pestic. Sci. 39 (1993) 131–140.
[8] A. Lucia, L.W. Juan, E.N. Zerba, L. Harrand, M. Marcó, H.M. Masuh, Validation of models to estimate the fumigant and larvicidal activity of Eucalyptus essential oils against Aedes aegypti (Diptera: Culicidae), Parasitol. Res. 110 (2012) 1675–1686.
[9] R. Pavela, Essential oils for the development of eco-friendly mosquito larvicides: a review, Ind. Crops Prod. 76 (2015) 174–187.
[10] J.-H. Tak, E. Jovel, M.B. Isman, Comparative and synergistic activity of Rosmarinus officinalis L. essential oil constituents against the larvae and an ovarian cell line of the cabbage looper, Trichoplusia ni (Lepidoptera: Noctuidae), Pest Manag. Sci. 72 (2016) 474–480.
[11] G.Q. Zeng, P.M. Kenney, L.K.T. Lam, Sesquiterpenes from clove (Eugenia caryophyllata), J. Nat. Prod. 55 (1992) 999–1003.
[12] C. Pasay, K. Mounsey, G. Stevenson, R. Davis, L. Arlian, M.V. Morgan, J. McCarthy, Acaricidal activity of eugenol based compounds against Scabies mites, PLoS One 5 (2010) e12079.
[13] E. Enan, Insecticidal activity of essential oils: octopaminergic sites of action, Comp. Biochem. Physiol. C 130 (2001) 325–337.
[14] K. Rhayour, T. Bouchikhi, T.E.A. Antaoui, K. Sendide, A. Remmal, The mechanism of bactericidal action of oregano and clove essential oils and of their phenolic major components on *Escherichia coli* and *Bacillus subtilis*, J. Essential Oil Res. 15 (2003) 286–292.
[15] A. de Amiri, R. Dugas, A.L. Pichot, G. Bompeix, In vitro and in vivo activity of eugenol oil (*Eugenia caryophylata*) against four important postharvest apple pathogens, Int. J. Food Microbiol. 126 (2008) 13–19.
[16] V. Zeringóta, T.O.S. Senra, F. Calmon, R. Mathurano, A.P. Faza, F.E.A. Catunda-Junior, C.M.O. Monteiro, M.G. de Carvalho, E. Daemon, Repellent activity of eugenol on larvae of*Rhipicephalus microplus* and *Dermacentor nitens* (Acari: Ixodidae), Parasitol. Res. 112 (2013) 2675–2679.
[17] M.L. Cornelius, J.K. Grace, J.R. Yates III, Toxicity of monoterpenoids and other natural products to the Formosan subterranean termite (Isoptera: Rhinotermitidae), J. Econ. Entomol. 90 (1997) 320–325.
[18] T. Tworkoski, Herbicide effects of essential oils, Weed Sci. 50 (2002) 425–431.
[19] D.P. De Sousa, Analgesic-like activity of essential oils constituents, Molecules 16 (2011) 2233–2252.
[20] I. Gulcin, Antioxidant activity of eugenol: a structure-activity relationship study, J. Med. Food 14 (2011) 975–985.
[21] M. Isman, Plant essential oils for pest and disease management, Crop. Prot. 19 (2000) 603–608.
[22] A. Lucia, Ariel C. Toloza, E. Guzmán, F. Ortega, R.G. Rubio, Novel polymeric micelles for insect pest control: encapsulation of essential oil monoterpenes inside a triblock copolymer shell for head lice control, PeerJ 5 (2017) e3171.
[23] B. Ali, N.A. Al-Wabel, S. Shams, A. Ahamad, S.A. Khan, F. Anwar, Essential oils used in aromatherapy: a systemic review, Asian Pac. J. Trop. Biomed. 5 (2015) 601–611.
[24] R. Botet, The "ouzo effect", recent developments and application to therapeutic drug carrying, J. Phys. 352 (2012) (2012) 012047.
[25] S. Schöttl, D. Touraud, W. Kunz, T. Zemb, D. Horinek, Consistent definitions of “the interface” in surfactant-free micellar aggregates, Colloids Surf. A 480 (2015) 222–227.
[26] H. Tan, C. Diddens, P. Lv, J.G.M. Kuerten, X. Zhang, D. Lohse, Evaporation-triggered microdroplet nucleation and the four life phases of an evaporating Ouzo drop, Proc. Nat. Acad. Sci. U.S.A. 113 (2016) 8642–8647.
[27] T.N. Zemb, M. Klossek, T. Lopian, J. Marcus, S. Schöettl, D. Horinek, S.F. Prevost, D. Touraud, O. Diat, S. Didier Touraud, W. Kunz, How to explain microemulsions formed by solvent mixtures without conventional surfactants, Proc. Nat. Acad. Sci. U.S.A. 113 (2016) 4260–4265.

[28] A. Lucia, P.G. Argudo, E. Guzmán, R.G. Rubio, F. Ortega, Formation of surfactant free microemulsions in the ternary system water/eugenol/ethanol, Colloids Surf. A 521 (2017) 133–140.
[29] S. Ribes, A. Fuentes, P. Talens, J.M. Barat, Use of oil-in-water emulsions to control fungal deterioration of strawberry jams, Food Chem. 211 (2016) 92–99.
[30] H. Cetin Babaoglu, A. Bayrak, N. Ozdemir, N. Ozgun, Encapsulation of clove essential oil in hydroxypropyl beta-cyclodextrin for characterization, controlled release, and antioxidant activity, J. Food Process. Preserv. 41 (2017) e13202.
[31] E. Santini, E. Guzmán, M. Ferrari, L. Liggieri, Emulsions stabilized by the interaction of silica nanoparticles and palmitic acid at the water–hexane interface, Colloids Surf. A 460 (2014) 603–608.
[32] B.P. Binks, Colloidal particles at a range of fluid-fluid interfaces, Langmuir 33 (2017) 6947–6963.
[33] A.J. Mendoza, E. Guzmán, F. Martínez-Pedrero, H. Ritacco, R.G. Rubio, F. Ortega, V.M. Starov, R. Miller, Particle laden fluid interfaces: dynamics and Interfacial rheology, Adv. Colloid Interface Sci. 206 (2014) 303–319.
[34] A. Maestro, E. Santini, D. Zabiegaj, S. Llamas, F. Ravera, L. Liggieri, F. Ortega, R.G. Rubio, E. Guzmán, Particle and particle-surfactant mixtures at fluid interfaces: assembly, morphology, and rheological description, Adv. Cond. Matt. Phys. 2015 (2015) 917516.
[35] C. Schmitt-Pauly, A.-C. Genix, J.G. Alauzun, J. Jestin, M. Sztucki, P.H. Mutin, J. Oberdisse, Structure of alumina-silica nanoparticles grafted with alkylphosphonic acids in poly(ethylacrylate) nanocomposites, Polymer 97 (2016) 138–146.
[36] D. Musino, A.-C. Genix, T. Chaussée, L. Guy, N. Meissner, R. Kozak, T. Bizien, J. Oberdisse, Aggregate formation of surface-modified nanoparticles in solvents and polymer nanocomposites, Langmuir 34 (2018) 3010–3020.
[37] J. Frelichowska, M.A. Bolzinger, J. Pelletier, J.P. Valour, Y. Chevalier, Topical delivery of lipophilic drugs from o/w Pickering emulsions, Int. J. Pharm. 371 (2009) 56–63.
[38] J. Frelichowska, M.A. Bolzinger, J.P. Valour, H. Mouaziz, J. Pelletier, Y. Chevalier, Pickering w/o emulsions: drug release and topical delivery, Int. J. Pharm. 368 (2009) 7–15.
[39] M. Bakshi, H.B. Singh, P.C. Abhilash, Unseen impact of nanoparticles: more or less? Curr. Sci. 106 (2014) 350–352.
[40] T.K.L. Barik, R. Kamaraju, A. Gowswami, Silica nanoparticle: a potential new insecticide for mosquito vector control, Parasitol. Res. 111 (2012) 1075–1083.
[41] A.A. El-Helaly, H.M. El-Bendary, A.S. Abdel-Wahab, M.A.K. El-Sheikh, S. Elnagar, The silica-nano particles treatment of squash foliage and survival and development of *Spodoptera littoralis* (Bosid.) larvae, J. Entomol. Zool. Stud. 4 (2016) 175–180.
[42] B. Plazzotta, E. Fegyver, R. Meszaros, J.S. Pedersen, Anisometric polyelectrolyte/mixed surfactant nanoassemblies formed by the association of poly(diallyldimethylammonium chloride) with sodium dodecyl sulfate and dodecyl maltoside, Langmuir 31 (2015) 7242–7250.
[43] S.V. Vlierberghe, E. Mendes, P. Dubruel, Cross-linkable, thermo-responsive Pluronic building blocks for biomedical applications: synthesis and physico-chemical evaluation, Eur Polymer J 53 (2014) 126–138.
[44] M. Malmsten, Soft drug delivery systems, Soft Matter 2 (2006) 760–769.
[45] M. Bohorquez, C. Koch, T. Trygstad, N. Pandit, A study of the temperature-dependent micellization of pluronic F127, J. Colloid Interface Sci. 216 (1999) 34–40.
[46] B. Sarkar, V. Venugopal, M. Tsianou, P. Alexandridis, Adsorption of Pluronic block copolymers on silica nanoparticles, Colloids Surf. A 422 (2013) 155–164.
[47] E.F. Voronin, V.M. Gun'ko, N.V. Guzenko, E.M. Pakhlov, L.V. Nosach, R. Leboda, J. Skubiszewska-Zieba, M.L. Malysheva, M.V. Borysenko, A.A. Chuiko, Interaction of poly(ethylene oxide) with fumed silica, J. Colloid Interface Sci. 279 (2004) 326–340.
[48] L. He, L. Zhang, H. Liang, The effects of nanoparticles on the lamellar phase separation of diblock copolymers, J. Phys. Chem. B 112 (2008) 4194–4203.
[49] P. Levitz, Aggregative adsorption of nonionic surfactants onto hydrophilic solid water interface. Relation with bulk micellization, Langmuir 7 (1991) 1595–1608.
[50] A. Milchev, K. Binder, Formation of surface micelles from adsorbed asymmetric block copolymers: a Monte Carlo study, Langmuir 15 (1999) 3232–3241.
[51] J.L. Escobar, D.M. García, D. Zaldivar, I. Katime, Hidrogeles. Principales características en el diseño de sistemas de liberación controlada de fármacos, Revista Iberoamericana de Polímeros 3 (2002) 83–94.
[52] M.G. Cueto, P.G. Audino, C.V. Vassena, M.I. Picollo, E.N. Zerba, Toxic effect of aliphatic alcohols against susceptible and permethrin-resistant *Pediculus humanus* capitis (Anoplura: Pediculidae), J. Med. Entomol. 39 (2002) 457–460.
[53] A. Toloza, C. Vassena, M.I. Picollo, Ovicidal and adulticidal effect of monoterpenoids against permethrin-resistant human head lice (Phthiraptera: Pediculidae), Med. Vet. Entomol. 45 (2008) 421–426.
[54] J.M. Taylor, P.M. Jenner, W.I. Jones, A comparison of the toxicity of some allyl, propenyl and propyl compounds in the rat, Toxicol. Appl. Pharmacol. 6 (1964) 378–387.
[55] P.M. Jenner, Food flavorings and compounds of related structure. I. Acute oral toxicity, Food Cosmet. Toxicol. 2 (1964) 327–343.